Supporting Information

Photophysical Probes to Assess the Potential of Cholic Acid Aggregates as Drug Carriers

Miguel Gomez-Mendoza, Edurne Nuin, Inmaculada Andreu, M. Luisa Marin and Miguel A. Miranda*

Instituto Universitario Mixto de Tecnología Química (UPV-CSIC), Universidad Politécnica de Valencia. Avenida de los Naranjos s/n, 46022 Valencia. Spain

	Page
1. Figures S1 a-b	S2
2. Figures S2 a-b	S3
3. Figures S3 a-i	S4, S5
4. Figures S4 a-d	S5
5. Figures S5 a-h	S6
6. Figures S6 a-d	S7
7. Figures S7 a-e	S8
8. Figures S8 a-d	S9
9. Figures S9 a-d	S10
10. Figures S10 a-d	S11
11. Figures S11 a-d	S12
12. Figures S12 a-c	S13
13. Figures S13 a-d	S14
14. Figures S14 a-c	S15
15. Photograph of fluorescence quenching by iodide	S16
16. Table of rate constants for fluorescence quenching by iodide	S17
17. Table of rate constants for triplet quenching by nitrite	S18

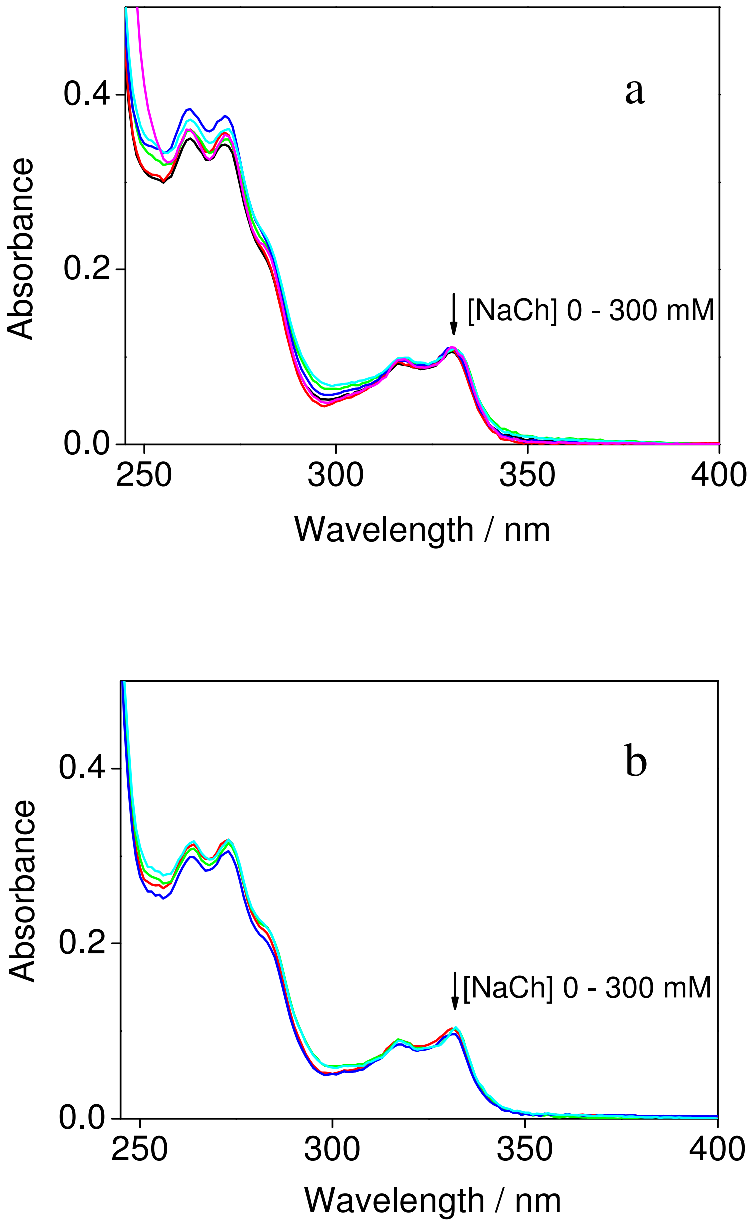

Figure S1. Absorption spectra of 60 μM solutions of (**a**) (*R*)- or (*S*)-NPX and (**b**) (*R*)- or (*S*)-NPXMe upon addition of increasing concentrations of sodium cholate in 0.2 M aqueous NaCl.

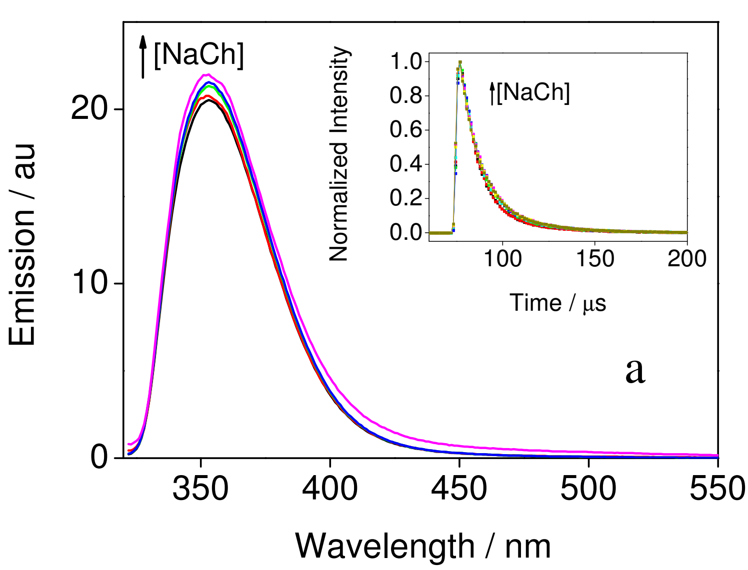

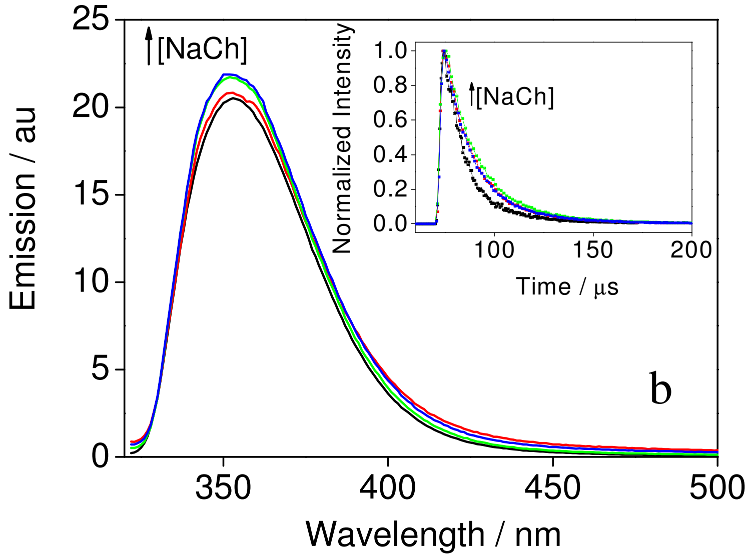

Figure S2. Emission spectra of (**a**) (*R*)- or (*S*)-NPX and (**b**) (*R*)- or (*S*)-NPX-Me *vs.* NaCh concentration up to 300 mM in 0.2 M aqueous NaCl. Insets: changes in the corresponding emission decay traces.

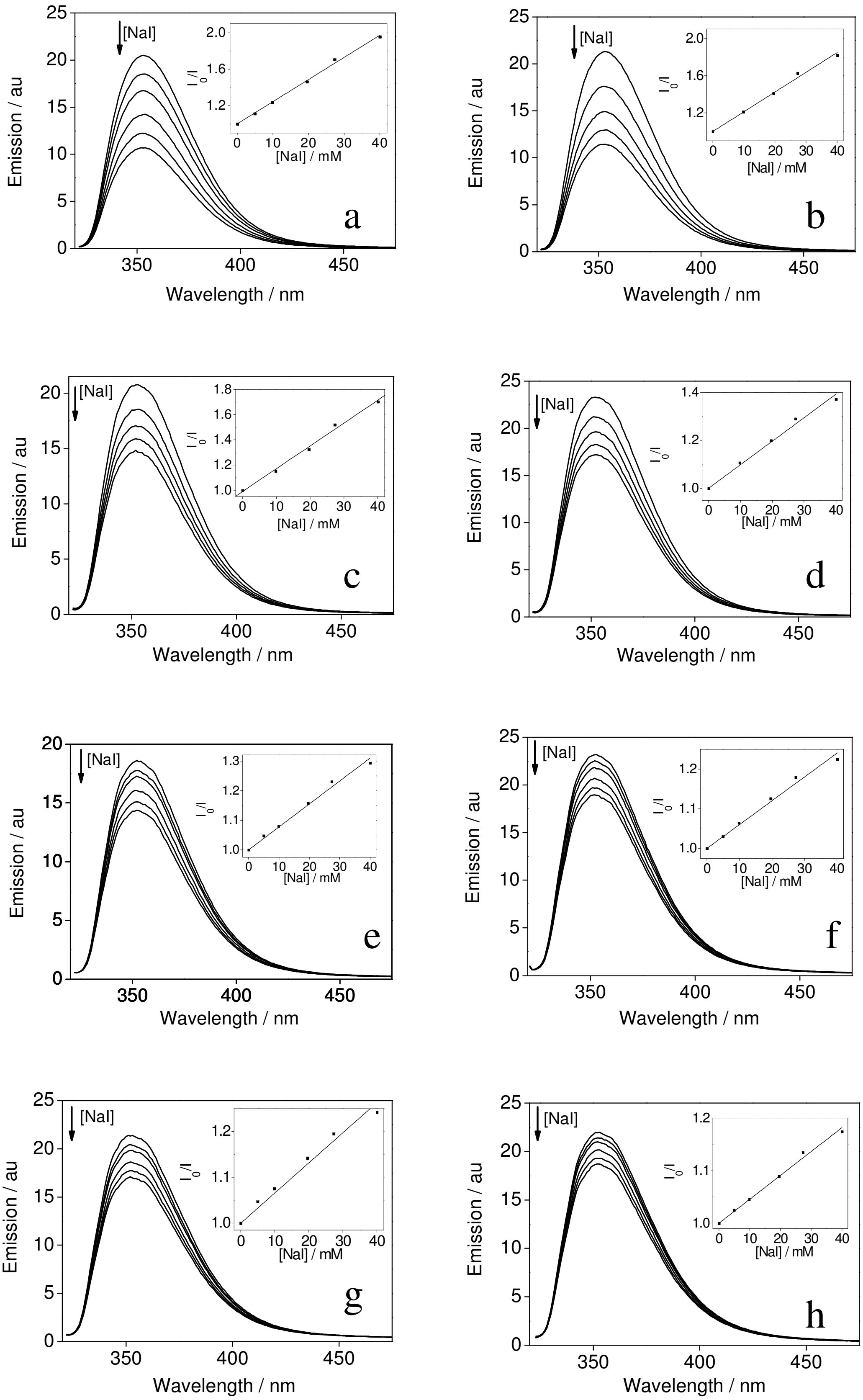
[NaI]
Emission / au
Wavelength / nm
I_0/I
[NaI] / mM
a
b
c
d
e
f
g
h

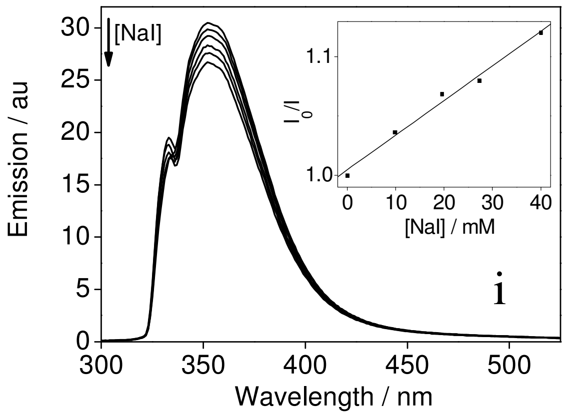

Figure S3. Emission spectra of (*R*)-NPX upon addition of increasing concentrations of NaI recorded in 0.2 M aqueous NaCl at different NaCh concentrations: **(a)** 0 mM; **(b)** 15 mM; **(c)** 50 mM; **(d)** 75 mM; **(e)** 100 mM; **(f)** 150 mM; **(g)** 200 mM; **(h)** 250 mM and **(i)** 300 mM. Insets: corresponding Stern-Volmer plots.

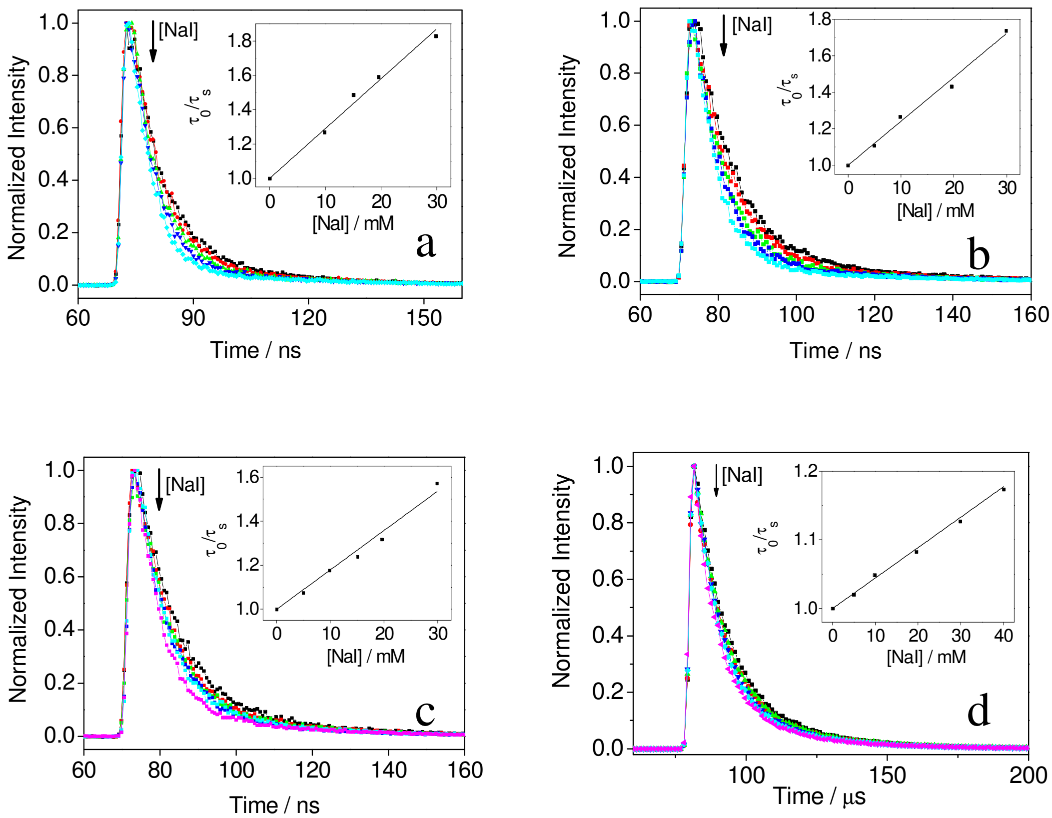

Figure S4. Changes in the emission decay traces of (*R*)-NPX in 0.2 M aqueous NaCl upon addition of increasing concentrations of NaI at different NaCh concentrations: **(a)** 0 mM; **(b)** 15 mM; **(c)** 50 mM and **(d)** 200 mM. Insets: corresponding Stern-Volmer plots.

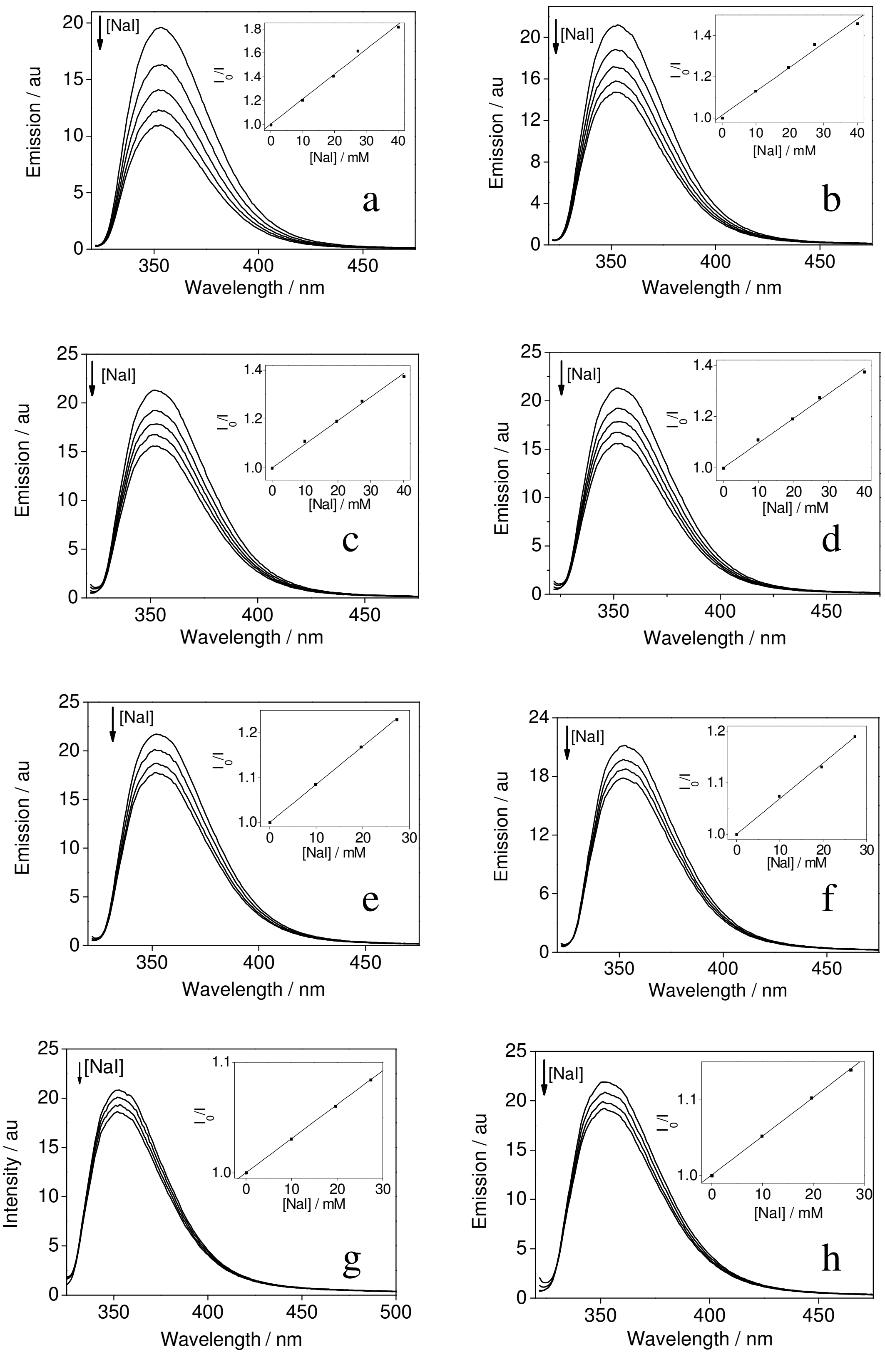

Figure S5. Emission spectra of (*S*)-NPX upon addition of increasing concentrations of NaI recorded in 0.2 M aqueous NaCl at different NaCh concentrations: **(a)** 0 mM; **(b)** 15 mM; **(c)** 50 mM; **(d)** 75 mM; **(e)** 100 mM; **(f)** 150 mM; **(g)** 200 mM and **(h)** 300 mM. Insets: corresponding Stern-Volmer plots.

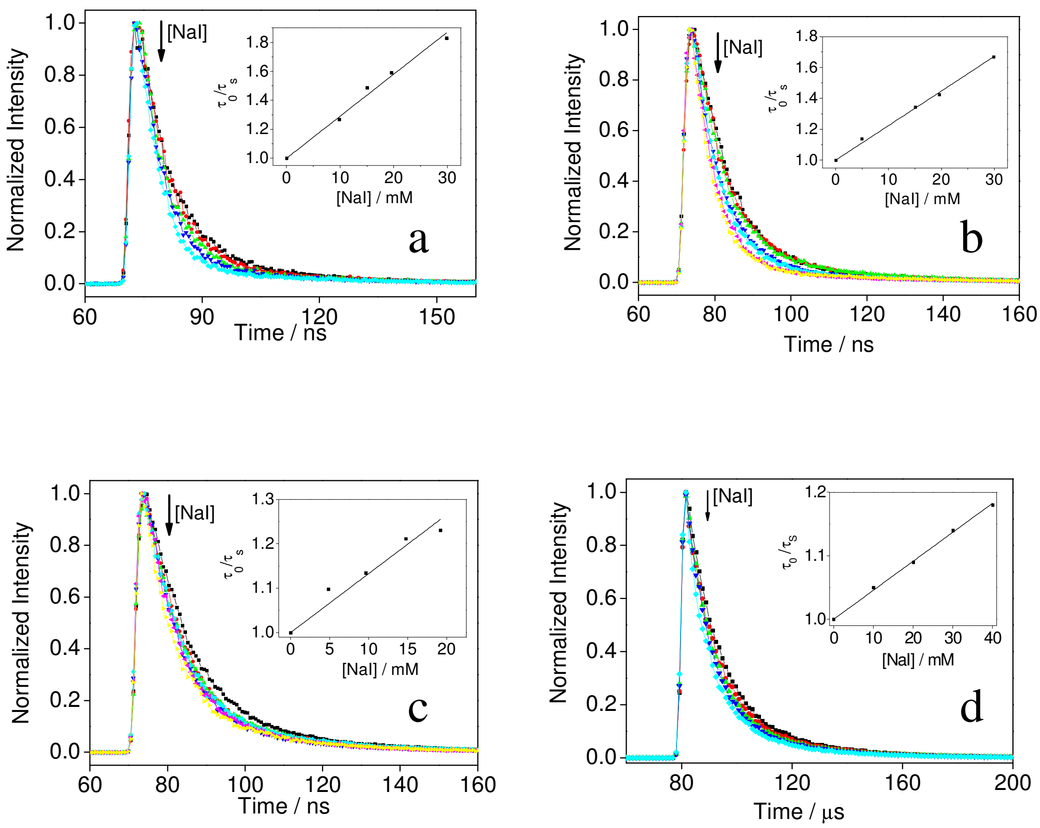

Figue S6. Changes in the emission decay traces of (*S*)-NPX in 0.2 M aqueous NaCl upon addition of increasing concentrations of NaI at different NaCh concentrations: **(a)** 0 mM; **(b)** 15 mM; **(c)** 50 mM and **(d)** 200 mM. Insets: corresponding Stern-Volmer plots.

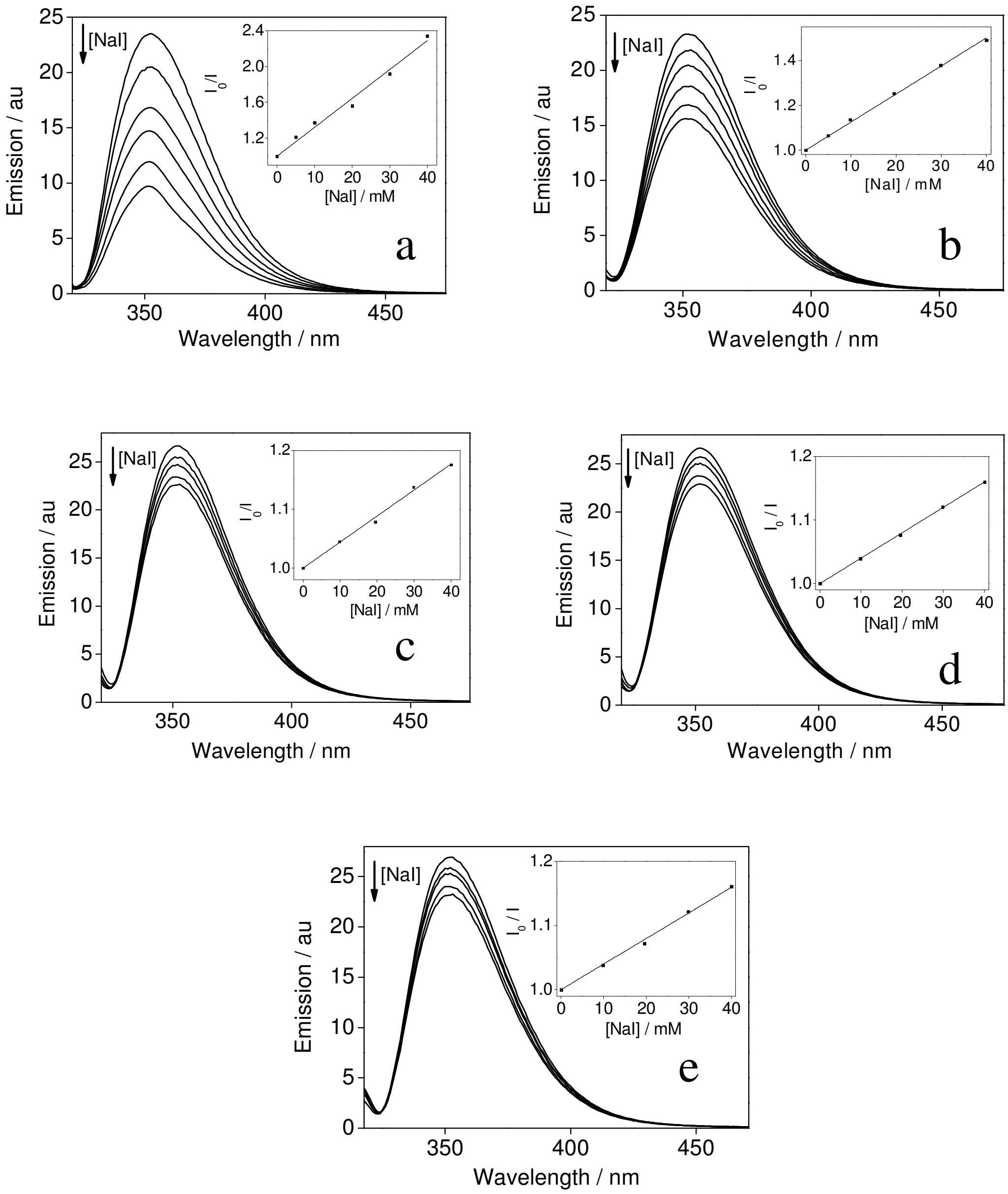

Figure S7. Emission spectra of (*R*)-NPXMe in 0.2 M aqueous NaCl upon addition of increasing concentrations of NaI at different NaCh concentrations: **(a)** 2 mM; **(b)** 15 mM and **(c)** 50 mM; **(d)** 200 mM and **(e)** 300 mM. Insets: corresponding Stern-Volmer plots.

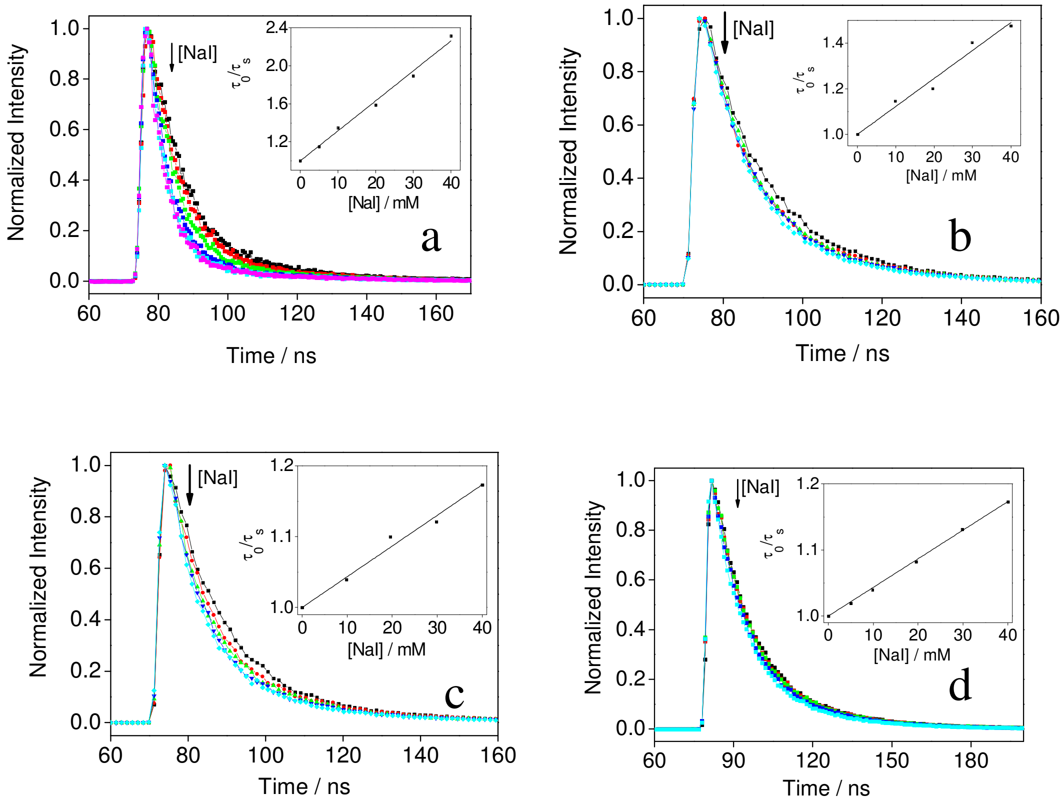

Figure S8. Changes in the emission decay traces of (*R*)-NPXMe in 0.2 M aqueous NaCl upon addition of increasing concentrations of NaI at different NaCh concentrations: **(a)** 2 mM; **(b)** 15 mM; **(c)** 50 mM and **(d)** 200 mM. Insets: corresponding Stern-Volmer plots.

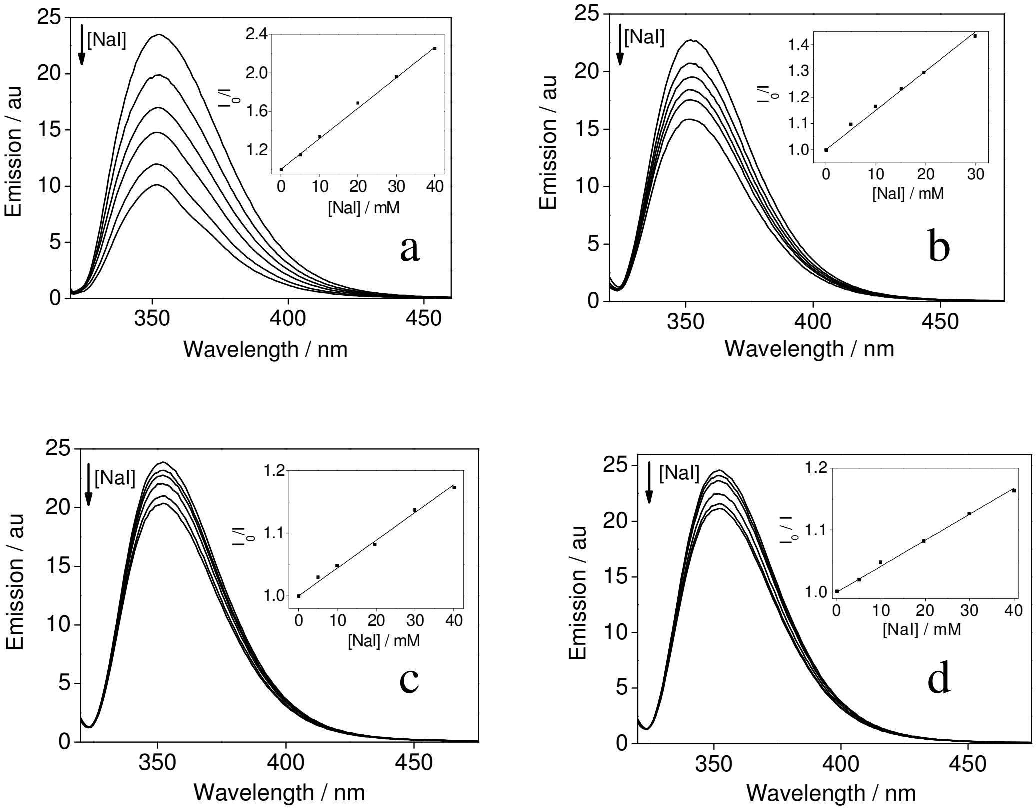

Figure S9. Emission spectra of (*S*)-NPXMe in 0.2 M aqueous NaCl upon addition of increasing concentrations of NaI at different NaCh concentrations: **(a)** 2 mM; **(b)** 15 mM; **(c)** 50 mM and **(d)** 300 mM . Insets: corresponding Stern-Volmer plots.

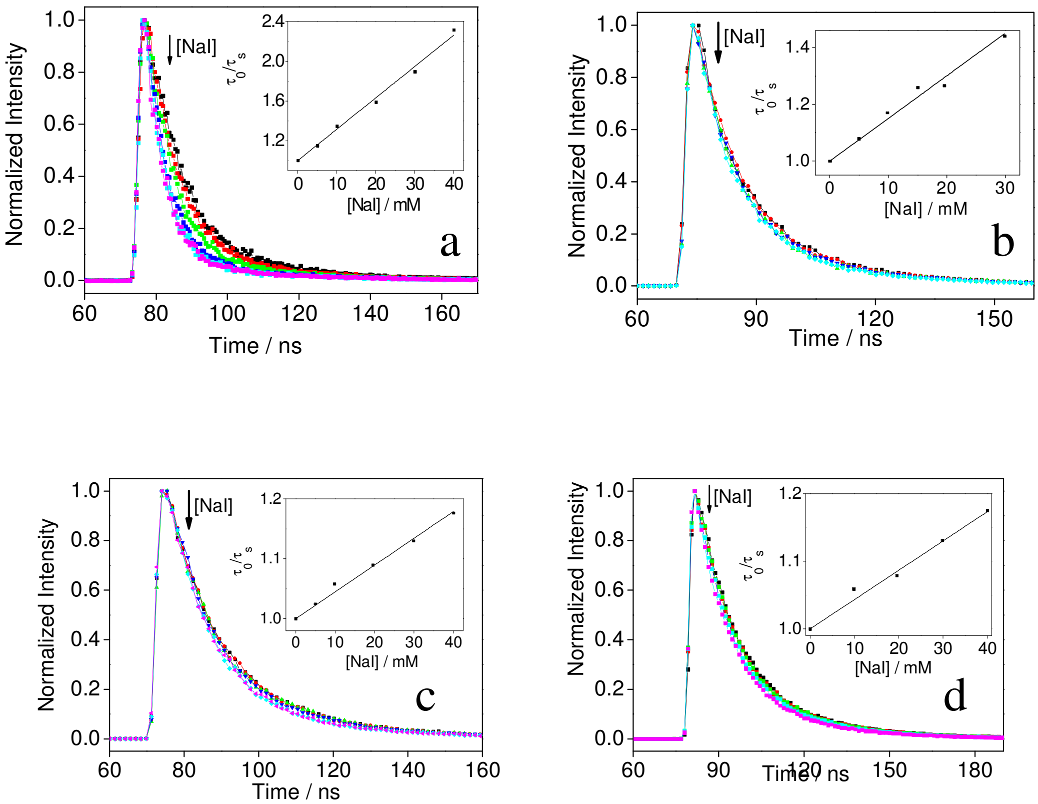

Figure S10. Changes in the emission decay traces of (*S*)-NPXMe in 0.2 M aqueous NaCl upon addition of increasing concentrations of NaI at different NaCh concentrations: **(a)** 2 mM; **(b)** 15 mM; **(c)** 50 mM and **(d)** 200 mM. Insets: corresponding Stern-Volmer plots.

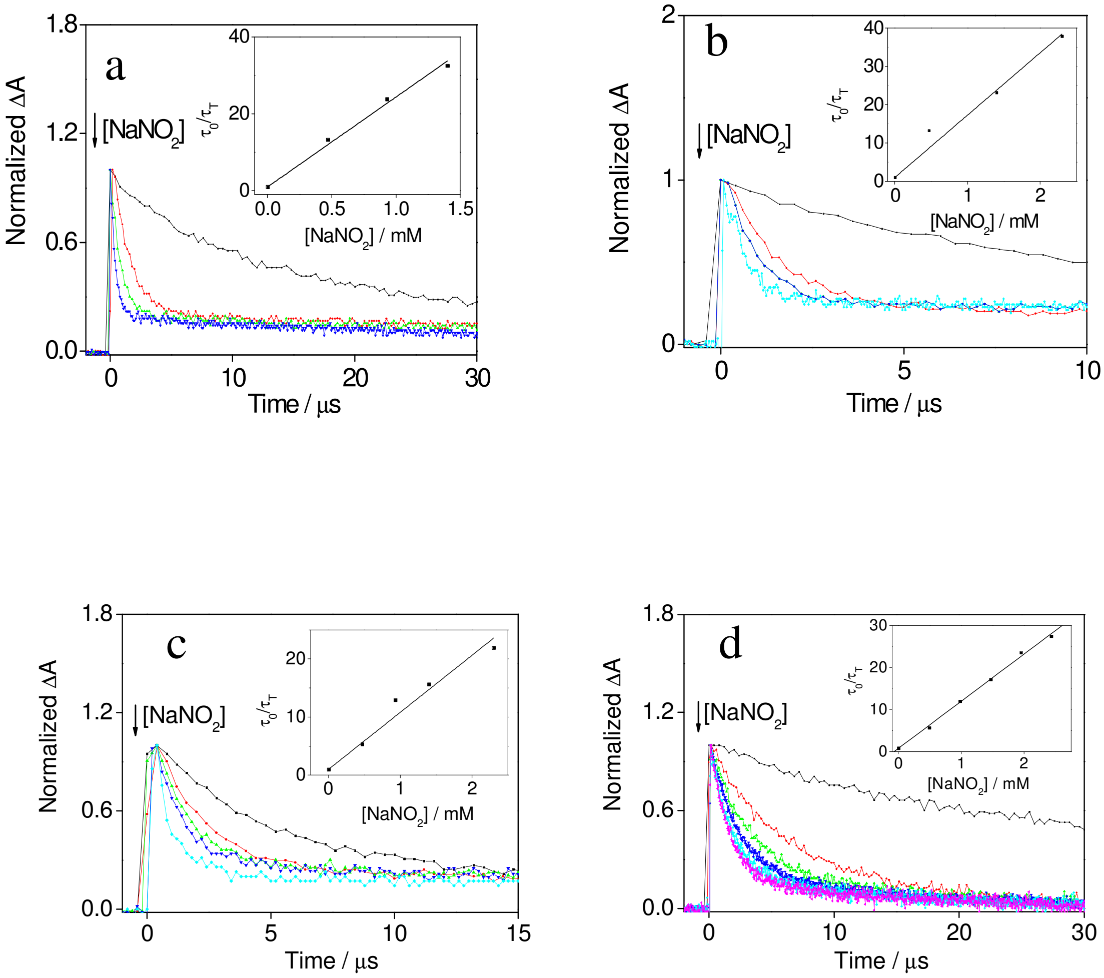

Figure S11. Changes in the triplet lifetime of (*R*)-NPX in deaerated 0.2 M aqueous NaCl, recorded at 440 nm upon addition of increasing volumes of $NaNO_2$ at different NaCh concentrations: **(a)** 0 mM; **(b)** 15 mM; **(c)** 50 mM and **(d)** 200 mM. Insets: corresponding Stern-Volmer plots. In all cases, the triplet decays were fitted to a mono-exponential function, with R^2 values higher than 0.98.

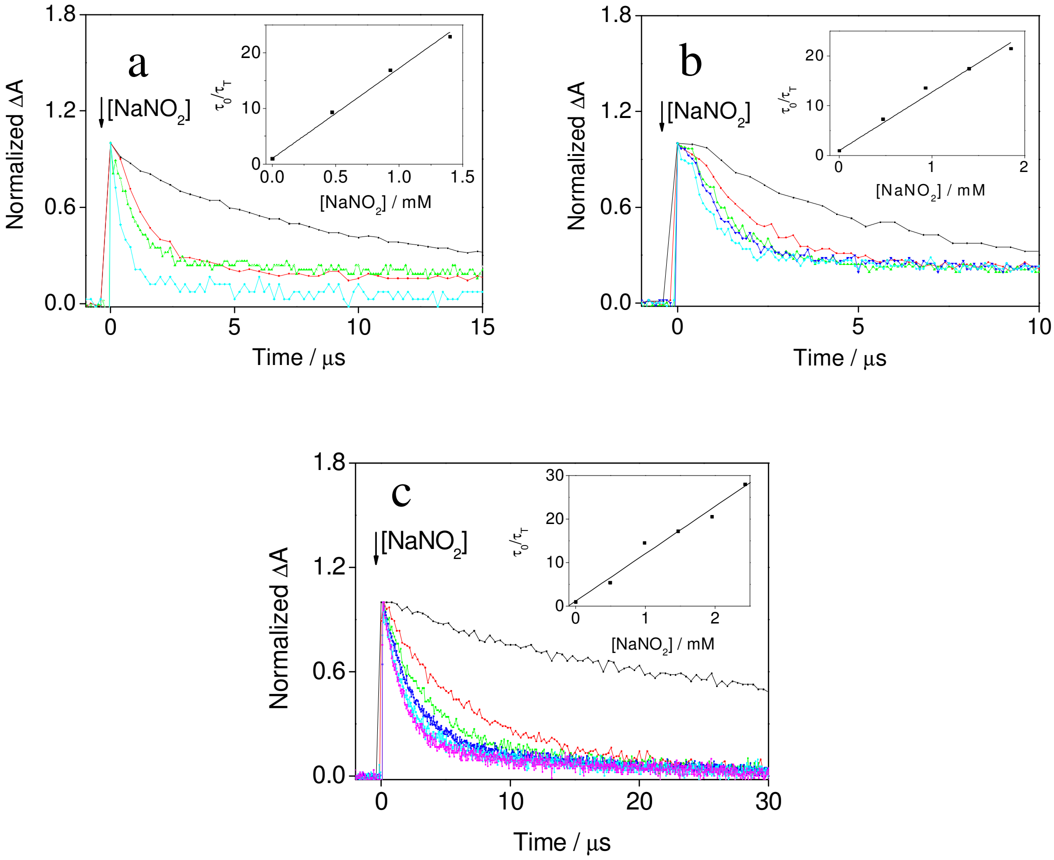

Figure S12. Changes in the triplet lifetime of (*S*)-NPX in deaerated 0.2 M aqueous NaCl, recorded at 440 nm upon addition of increasing volumes of $NaNO_2$ at different NaCh concentrations: **(a)** 15 mM; **(b)** 50 mM and **(c)** 200 mM. Insets: corresponding Stern-Volmer plots. In all cases, the triplet decays were fitted to a mono-exponential function, with R^2 values higher than 0.98.

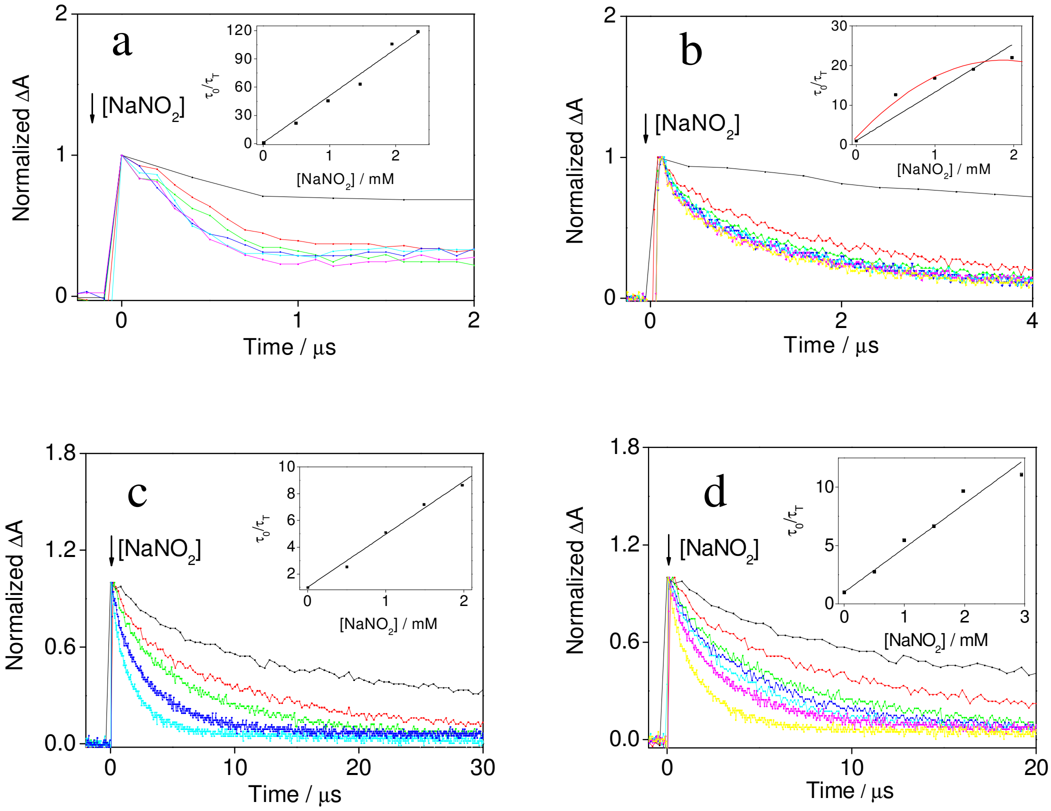

Figure S13. Changes in the triplet decay traces of (*R*)-NPXMe in deaerated 0.2 M aqueous NaCl, recorded at 440 nm upon addition of increasing concentrations of $NaNO_2$ at different NaCh concentrations: **(a)** 2 mM; **(b)** 15 mM; **(c)** 50 mM and **(d)** 200 mM. Insets: corresponding Stern-Volmer plots; in the case of **(b)**, in addition to the linear fitting (black), the curved plot was fitted to eqn. (2) of page S18 (red). In all cases, the triplet decays were fitted to a mono-exponential function, with R^2 values higher than 0.98.

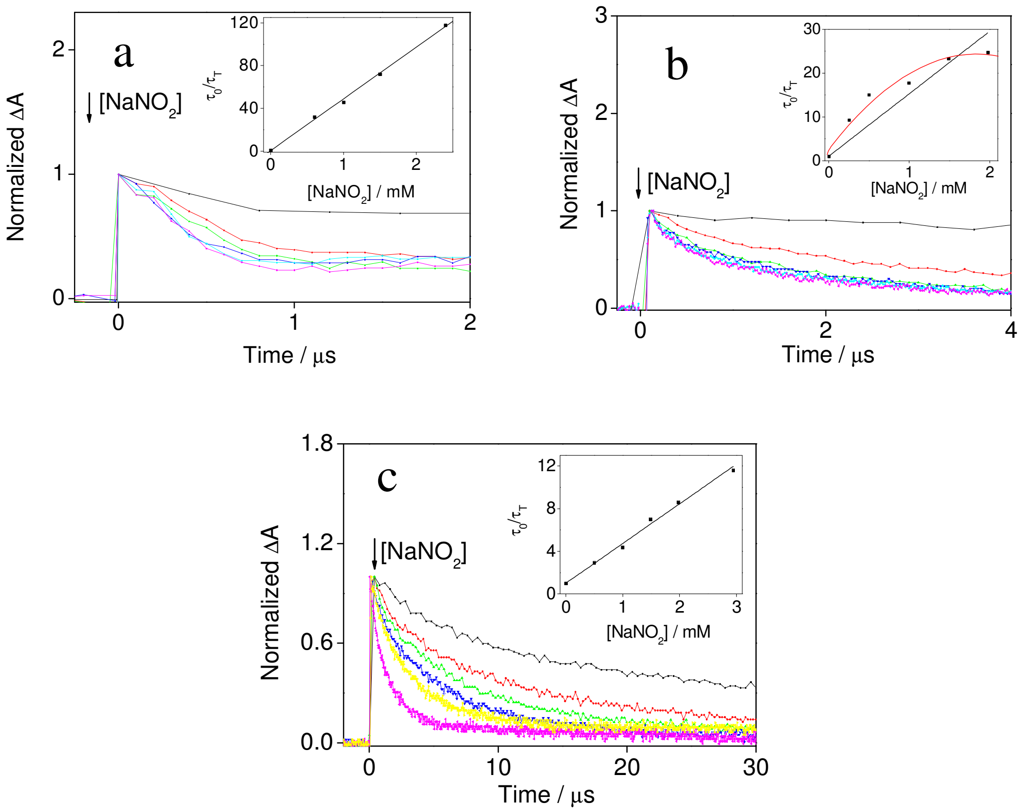

Figure S14. Changes in the triplet decay traces of (*S*)-NPXMe in deaerated 0.2 M aqueous NaCl, recorded at 440 nm upon addition of increasing concentrations of $NaNO_2$ at different NaCh concentrations: **(a)** 2 mM, **(b)** 15 mM and **(c)** 50 mM. Insets: corresponding Stern-Volmer plots; in the case of **(b)**, in addition to the linear fitting (black), the curved plot was fitted to eqn. (2) of page S18 (red). In all cases, the triplet decays were fitted to a mono-exponential function, with R^2 values higher than 0.98.

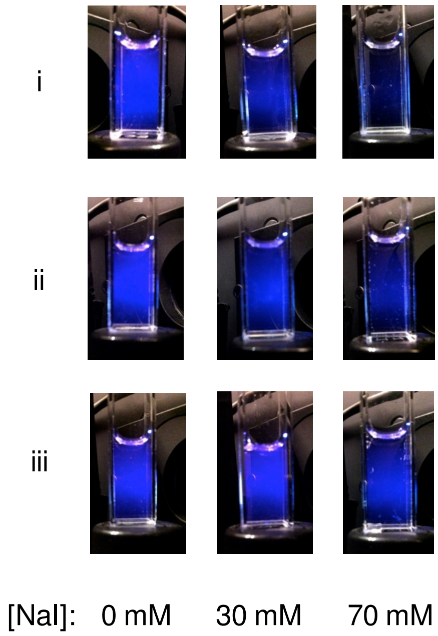

Figure S15. Fluorescence quenching by iodide for (i) (*S*)-NPX in 0.2 M aqueous NaCl solution; (ii) same as (i) in the presence of 50 mM NaCh and (iii) (*S*)-NPXMe in 0.2 M aqueous NaCl solution and in the presence of 50 mM NaCh.

Table 1. Rate constants for fluorescence quenching by iodide.

[NaCh] / mM	k_q^S / 10^9 ($M^{-1}s^{-1}$) [a] (S)-NPX Steady-State	(S)-NPX Time-Resolved	(S)-NPX % Bound[b]	(R)-NPX Steady-State	(R)-NPX Time-Resolved	(R)-NPX % Bound[b]	(S)-NPXMe Steady-State	(S)-NPXMe Time-Resolved	(S)-NPXMe % Bound[b]	(R)-NPXMe Steady-State	(R)-NPXMe Time-Resolved	(R)-NPXMe % Bound[b]
0	2.40 ± 0.04	2.90 ± 0.09	0	2.40 ± 0.04	2.90 ± 0.09	0	4.43[c]	--	0	4.43[c]	--	0
2	--	--	--	--	--	--	3.30 ± 0.11	3.30 ± 0.08	27	3.30 ± 0.11	3.30 ± 0.08	27
15	2.10 ± 0.05	2.00 ± 0.04	14	2.20 ± 0.05	2.40 ± 0.07	9	1.25 ± 0.03	1.20 ± 0.04	77	0.98 ± 0.01	0.97 ± 0.04	83
50	1.09 ± 0.03	1.10 ± 0.07	62	1.60 ± 0.04	1.60 ± 0.06	37	0.31 ± 0.01	0.32 ± 0.04	99	0.32 ± 0.01	0.31 ± 0.01	99
75	0.87 ± 0.02	--	73	0.87 ± 0.03	--	71	--	--	--	--	--	--
100	0.71 ± 0.01	--	80	0.67 ± 0.02	--	81	--	--	--	--	--	--
150	0.53 ± 0.01	--	89	0.50 ± 0.02	--	89	--	--	--	--	--	--
200	0.41 ± 0.01	0.38 ± 0.01	94	0.43 ± 0.03	0.38 ± 0.01	92	--	0.32 ± 0.01	--	0.27 ± 0.01	0.29 ± 0.04	100
250	--	--	--	0.37 ± 0.01	--	95	--	--	--	--	--	--
300	0.29 ± 0.01	--	100	0.26 ± 0.01	--	100	0.27 ± 0.01	--	100	0.27 ± 0.01	--	100

[a] The experiments were perfomed twice and the errors correspond to average deviations.

[b] Percentage of bound drug (100X) estimated as:

$$k_q^s = X \cdot k_q^s(at\ 300\ mM\ NaCh) + (1-X) \cdot k_q^s(at\ 0\ mM\ NaCh) \qquad (1)$$

[c] Extrapolated.

Table 2. Rate constants for triplet quenching by nitrite.

k_q^T / 10^9 ($M^{-1}s^{-1}$) [a]				
[NaCh] / mM	(*S*)-NPX	(*R*)-NPX	(*S*)-NPXMe	(*R*)-NPXMe
0	1.50 ± 0.03	1.50 ± 0.03	--	--
2	--	--	2.30 ± 0.10	2.30 ± 0.08
15	0.82 ± 0.02	0.92 ± 0.04	0.42 ± 0.05 *	0.48 ± 0.05 *
50	0.38 ± 0.03	0.52 ± 0.04	0.11 ± 0.01	0.13 ± 0.01
200	0.20 ± 0.01	0.21 ± 0.01	--	0.21 ± 0.01

[a] The experiments were perfomed twice and the errors correspond to average deviations.

* At this NaCh concentration, quenching plots were curved. Hence, the data were also analyzed using the model previously described in the literature[8], using eqn. 2:

$$k_{obs} = k_0^{BSa} + k_{dis} + k_q^{BSa}[Q] - \frac{k_{dis} k_{as} \frac{[NaCh]}{N}}{k_{as} \frac{[NaCh]}{N} + k_0 + k_q[Q]} \quad (2)$$

where k_0 and k_0^{BSa} are the decay rate constants in the absence of quencher of the guest in solution and in the presence of bile salt aggregate, respectively, k_q and k_q^{BSa} are the quenching rate constants for the triplet excited state in solution and when bound to the bile salt aggregate, respectively, k_{as} and k_{dis} are the association and dissociation rate constants of the triplet guest with the host, and [NaCh]/*N* corresponds to the concentration of binding sites in the aggregate, being [NaCh] the bile salt monomer concentration and *N* the aggregation number.

Applying the above model in the cases where quenching plots are curved, the rate constants determined for triplet quenching by nitrite were 0.20 ± 0.02 and 0.19 ± 0.01 x 10^9 ($M^{-1}s^{-1}$) for (*S*)-NPXMe and (*R*)-NPXMe, respectively.